

CLUSTERS OF GALAXIES AS SELF-GRAVITATING SYSTEMS

Florence DURRET

Institut d'Astrophysique de Paris, 98bis Bd Arago, 75014 Paris, France

Ricardo DEMARCO

ESO, Karl Schwarzschild Str. 2, Garching bei München, Germany
Institut d'Astrophysique de Paris, 98bis Bd Arago, 75014 Paris, France

Frédéric MAGNARD

Institut d'Astrophysique de Paris, 98bis Bd Arago, 75014 Paris, France

Daniel GERBAL

Institut d'Astrophysique de Paris, 98bis Bd Arago, 75014 Paris, France

Self-gravitating systems such as elliptical galaxies appear to have a constant specific entropy and obey a scaling law relating their potential energy to their mass. These properties can be interpreted as due to the physical processes involved in the formation of these structures. Dark matter haloes obtained through numerical simulations have also been found to obey a scaling law relating their potential energy to their mass with the same slope as ellipticals. Since the X-ray gas in clusters is weakly dissipative, we have checked the hypothesis that it might verify similar properties.

We have analyzed ROSAT-PSPC images of 24 clusters, and also found that: 1) the Sérsic law parameters (intensity, shape and scale) describing the X-ray gas emission are correlated two by two; 2) the hot gas in all these clusters roughly has the same specific entropy; 3) a scaling law linking the cluster potential energy to the mass of the X-ray gas is observed, with the same slope as for elliptical galaxies and dark matter haloes.

1 Introduction

The optical surface brightness profiles of elliptical galaxies can be fit by a Sérsic law (Sérsic 1968):

$$\Sigma(s) = \Sigma_0 \exp \left[- \left(\frac{s}{a} \right)^\nu \right] \quad (1)$$

characterized by three parameters: Σ_0 (intensity), a (scaling) and ν (shape). We have shown for a sample of 132 ellipticals belonging to three clusters that the Sérsic parameters were correlated two by two, and that in the three-dimensional space defined by these three parameters they were located on a thin line (Fig. 1). These properties have been interpreted as due to the fact that, to a first approximation, all these elliptical galaxies have the same specific entropy (entropy per unit mass) (Gerbal et al. 1997, Lima Neto et al. 1999, Márquez et al. 2000), and that a scaling law exists between the potential energy U and the mass M for these galaxies (Márquez et al. 2001): $U \propto M^{1.72 \pm 0.03}$. Each of these relations defines a two-manifold in the $[\log \Sigma_0, \log a, \nu]$ space. The thin line on which the galaxies are distributed in this space is the intersection of these

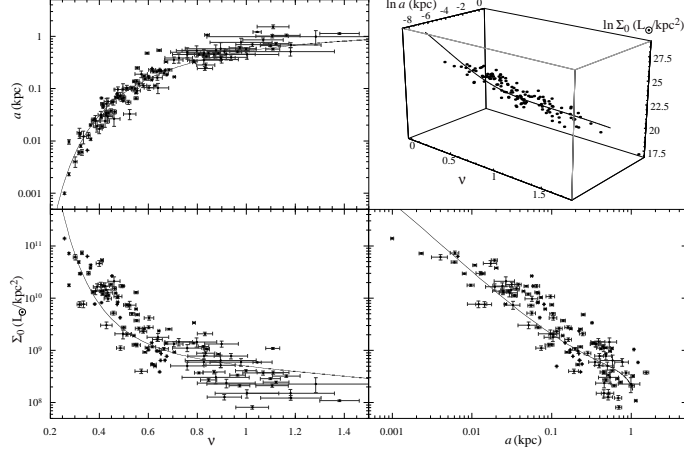


Figure 1: Two by two correlations of the Sérsic parameters $\log \Sigma_0, \log a, \nu$ for elliptical galaxies. Distribution of elliptical galaxies in the 3D Sérsic parameter space (top right). The lines superimposed in each panel are the correlations predicted from the intersection of the Entropic Surface (constant specific entropy) and Potential energy-mass relation scaling relation.

two two-manifolds (Fig. 2). Such relations are most probably a consequence of the formation and evolution processes undergone by these objects, since theory predicts $U \propto M^{5/3}$ under the hypothesis that energy and mass are conserved (Márquez et al. 2001).

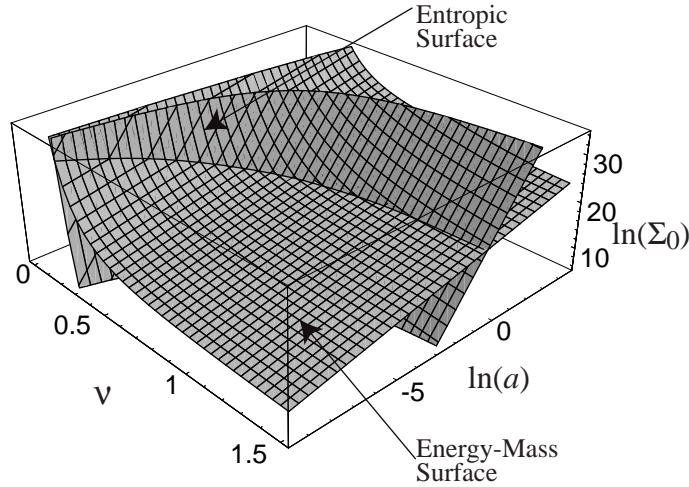


Figure 2: 3D representation of the specific entropy and potential energy-mass two-manifolds for elliptical galaxies, using the coordinates $[\log \Sigma_0, \log a, \nu]$.

Interestingly, numerical simulations of cold dark matter haloes in two different mass ranges lead to a similar scaling law between the potential energy and mass of the haloes. In the mass range $4 \cdot 10^5 \leq M \leq 4 \cdot 10^8 M_\odot$ (unvirialized clusters), Jang Condell & Hernquist (2001) find a relation consistent with $U \propto M^{5/3}$, while in the mass range $10^{12} \leq M \leq 10^{15} M_\odot$ (virialized clusters), Lanzoni (2000) finds $U \propto M^{1.69 \pm 0.02}$.

Since the X-ray gas in clusters of galaxies is weakly dissipative, it is likely to verify similar properties. The work presented here is meant to check this hypothesis. Our results are still preliminary and will be fully presented in a forthcoming paper (Demarco et al. in preparation).

2 The data and data reduction

We have selected a sample of 24 clusters with redshifts between 0.01 and 0.3 from the ROSAT PSPC archive with a high exposure time (and therefore signal to noise ratio), a roughly regular structure (obviously interacting clusters were discarded) and a proper light curve (no count rate peaks larger than 3 counts/seg in the 4 bands used). The main properties of the selected clusters are given in Table 1.

Table 1: Physical parameters of the 24 clusters of our sample.

Cluster	z	ν	$a(kpc)$	$a_{eq}(kpc)$	$n_{e0}(cm^{-3})$	$p(\nu)$	$r_{eff}(kpc)$	$T_0(keV)$
A85	0.0518	0.55	278	252	0.00581	0.68	2939	6.20
A478	0.0881	0.50	155	138	0.01600	0.71	2572	6.90
A644	0.0704	0.82	427	371	0.00365	0.54	1216	6.59
A1651	0.0860	0.74	411	373	0.00391	0.58	1597	6.10
A1689	0.1810	0.58	208	193	0.01407	0.67	1877	9.02
A1795	0.0631	0.54	178	157	0.01314	0.68	1939	5.88
A2029	0.0765	0.49	164	145	0.01717	0.71	2839	8.47
A2034	0.1510	1.00	868	784	0.00179	0.45	1740	7.00
A2052	0.0348	0.47	108	96	0.01245	0.72	2359	3.10
A2142	0.0899	0.81	601	495	0.00401	0.54	1686	9.70
A2199	0.0299	0.60	192	175	0.00733	0.65	1451	4.10
A2219	0.2250	0.85	737	667	0.00295	0.52	2017	12.40
A2244	0.0970	0.56	237	237	0.00724	0.67	2586	8.47
A2319	0.0559	0.80	801	733	0.00197	0.55	2570	9.12
A2382	0.0648	1.17	904	797	0.00057	0.36	1398	5.00
A2390	0.2310	0.59	347	297	0.00776	0.66	2593	11.10
A2589	0.0416	0.72	345	297	0.00253	0.59	1373	3.70
A2597	0.0852	0.34	20.6	18	0.17712	0.80	3763	4.40
A2670	0.0761	0.52	219	213	0.00407	0.70	3127	4.45
A2744	0.3080	1.35	949	843	0.00208	0.28	1246	11.00
A3266	0.0594	1.18	999	905	0.00126	0.36	1569	8.00
A3667	0.0552	0.89	1143	921	0.00107	0.50	2548	7.00
A3921	0.0960	0.81	762	604	0.00150	0.54	2036	4.90
A4059	0.0460	0.64	254	222	0.00462	0.64	1479	3.97

The data reduction was done using Snowden's now standard software (Snowden et al., 1994).

3 The method

3.1 Fitting the Sérsic parameters

In order to model the X-ray emission of the cluster, we have chosen a 3D density profile $\rho(r)$, which is a generalized form of a Mellier-Mathez profile (Mellier & Mathez 1987). It is completely determined by its three parameters and can be written under the form:

$$\rho(r) = \rho_0 (r/a)^{-p} \exp[-(r/a)^\nu] \quad (2)$$

where the parameters p and ν are related by the numerical approximation (Márquez et al. 2001):

$$p \simeq 1.0 - 0.6097\nu + 0.05563\nu^2 \quad (3)$$

This relation gives the best approximation to the Sérsic law when equation (2) is projected. The Sérsic profile defined by equation (1) corresponds to a surface mass density while equation (2) is the volume mass density. The condition that the mass obtained by integrating equation (1) must be equal to the mass obtained by integrating equation (2), gives us the following relation between the parameters Σ_0 and ρ_0 :

$$\rho_0 = \frac{1}{a} \Sigma_0 \frac{\Gamma(\frac{2}{\nu})}{2 \Gamma(\frac{3-p}{\nu})} \quad (4)$$

where $\Gamma(a)$ is the gamma function defined by $\Gamma(a) = \int_0^\infty x^{a-1} e^{-x} dx$.

In order to determine the correct set of values for the three Sérsic parameters for each cluster, we fit the ROSAT images by a pixel-to-pixel method which: i) creates a three-dimensional model of the X-ray emission and ii) projects it by integration along the line of sight, taking into account the energy response and the point spread function of the detector. The result is a synthetical image which can be compared with the observation.

To obtain this synthetical image, we have used a code that takes into account the generalized Mellier-Mathez density profile (equation (2)) and not only the free-free Bremsstrahlung emission, but also the free-bound and bound-bound X-ray emissions. The code computes the X-ray emissivity, ϵ_ν , in every point of the space; this emissivity is then projected by integration along the line of sight to obtain a surface brightness:

$$\mu(s) = \int_{z=-\infty}^{+\infty} \int_{\nu_{min}}^{\nu_{max}} \epsilon_\nu(s^2 + z^2) w(\nu) d\nu dz$$

where $s^2 = x^2 + y^2$, with x and y the perpendicular directions to the line of sight, and z the coordinate along the line of sight. This integral is computed taking into account the energy response of the satellite $w(\nu)$.

Finally, this projected image is convolved with the ROSAT point spread function (PSF), which varies as a function of position on the detector and energy. We have used a FWHM of 2 pixels which corresponds to the central PSF, because the resulting spreading is more important in the center where the intensity gradient is stronger.

The cluster redshift and the gas temperature are required as input parameters. The redshift for each cluster was taken from the SIMBAD data base (except for A2199 for which the redshift was obtained from Wu, Xue & Fang (1999), and the gas temperature was taken from Wu, Xue & Fang (1999), except for A2034 for which the temperature was taken from Ebeling et al. (1996), and for A2382 for which we have used a temperature of 5.0 keV. We assumed a standard CDM cosmology with a Hubble constant $H_0 = 50 \text{ km s}^{-1} \text{ Mpc}^{-1}$, $\Omega_0 = 1$, and $\Lambda = 0$.

To obtain an initial guess for the free parameters in equation (2) we fit a Sérsic profile (equation (1)) to the X-ray surface brightness of each cluster. The ellipticity and semi-major axis position angle of the X-ray gas were also given as starting values for the code.

Once we have obtained the first synthetic image with the initial guess for the value of each free parameter, the code compares it to the actual ROSAT image. The values of the parameters are then changed and the comparison process is repeated iteratively, until it finds the 3D X-ray emission (density dependent) which best fits the surface brightness profile of the observation when projected. The fitting process is carried out with the MIGRAD methode in the MINUIT library of CERN (James 1994).

The best fit parameters for each cluster are: the semi-major axis a (in kpc), the shape parameter ν (dimensionless) and the central electronic number density, n_{e0} (cm^{-3}).

Since the formula used to calculate the specific entropy is valid only for spherical symmetry, and in order to take the ellipticity of the X-ray emission into account, we have also computed

a new scale parameter, a_{eq} , defined by $a_{eq} = a \sqrt{b/a}$. In this way, we will calculate the specific entropy of a spherically symmetric X-ray region with a scale parameter a_{eq} . The best fit parameters are given in Table 1.

3.2 Calculation of the various physical quantities

By integrating equation (2) we find the gas mass as a function of radius:

$$M_{gas}(r) = \int_0^r \rho(u) 4\pi u^2 du = \frac{4\pi\rho_0 a^3}{\nu} \gamma\left(\frac{3-p}{\nu}, \left(\frac{r}{a}\right)^\nu\right) \quad (5)$$

where $\gamma(a, z)$ is the incomplete gamma function defined by $\gamma(a, z) = \int_0^z x^{a-1} e^{-x} dx$.

In order to estimate the total gas mass, we only have to integrate the last equation until $r = \infty$ (note that $\rho(r)$ does not diverge). The result is:

$$M_{gas} = 2\pi a^2 \Sigma_0 \frac{1}{\nu} \Gamma\left(\frac{2}{\nu}\right) \quad (6)$$

which depends only on the free parameters of the Sérsic law. The potential energy of the gas is given by:

$$U_{pot} \equiv \frac{M_{gas}^2}{R_g} = 4\pi^2 a^3 \Sigma_0^2 \frac{\left(\frac{1}{\nu} \Gamma\left(\frac{2}{\nu}\right)\right)^2}{R_g^*} \quad (7)$$

where we have used a gravitational constant $G = 1$ and where the gravitational radius R_g is defined by $R_g = a R_g^*$. Here a is the scale parameter and R_g^* is a dimensionless radius given by the numerical approximation: $\ln(R_g^*) \simeq \frac{0.82032 - 0.92446 \ln(\nu)}{\nu} + 0.84543$ (Márquez et al. 2001).

The second principle of thermodynamics states that a dynamical system in an equilibrium state has a maximum entropy. For a self-gravitating system in quasi-equilibrium, such as a galaxy cluster, there is no state with an entropy maximum. On the contrary, the entropy is constantly growing, but slowly, in a secular time scale, during which we can consider it as nearly constant. In spite of the X-ray emission, which is responsible in many cases for cooling flow processes which affect the equilibrium state of the cluster, we may therefore consider these objects as structures where dissipation processes are negligible compared to their gravitational energy, thus settling into a thermodynamical equilibrium.

The specific entropy of the intra-cluster gas can be obtained from the distribution function in the phase space, $f(\vec{x}, \vec{v})$, of the gas particles. The calculation is made using the microscopic Boltzmann-Gibbs definition:

$$s = \frac{S}{M_{gas}} = \frac{\int f \ln(f) d^3x d^3v}{\int f d^3x d^3v} \quad (8)$$

Estimating the distribution function f may be very difficult and some hypotheses are needed to simplify the problem. The first hypothesis is that our system has spherical symmetry, and the second one is that the velocity dispersion of the gas particles is isotropic. With these assumptions we are neglecting any possible rotation of the gas, and f can be obtained by Abel inversion from the density profile (Binney & Tremaine, 1987). Using equations (2) and (4), the gas specific entropy (Lima Neto et al., 1999; Márquez et al., 2000) is then:

$$s = \frac{3}{2} \ln \Sigma_0 + \frac{9}{2} \ln a + F(\nu) \quad (9)$$

where F is a function of the ν parameter given by the numerical approximation:

$$F(\nu) \simeq -0.795 \ln(\nu) - \frac{1.34}{\nu} + 3.85 \left(\frac{1}{\nu}\right)^{1.29} + \ln\left(\Gamma\left[\frac{2}{\nu}\right]\right) - 0.822$$

4 Results

4.1 Correlation of the Sérsic parameters two by two

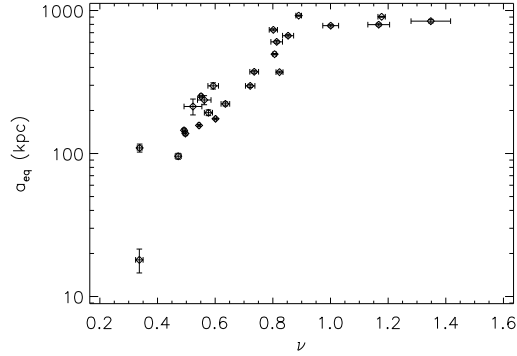


Figure 3: Correlation between the shape and scale parameters.

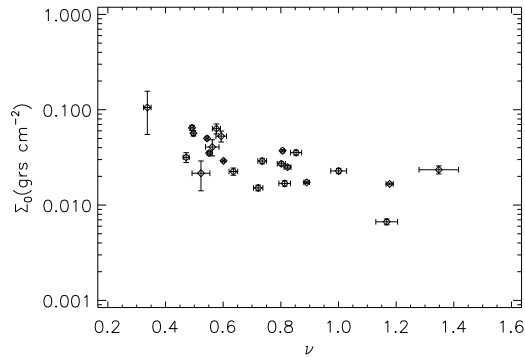


Figure 4: Correlation between the shape and intensity parameters.

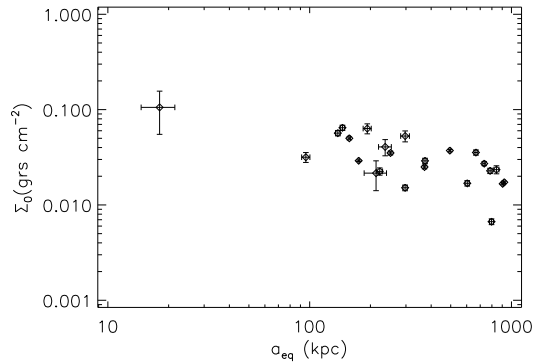


Figure 5: Correlation between the scale and intensity parameters.

We see in Figs. 3, 4 and 5 that the three Sérsic parameters are correlated two by two, as was previously observed for the optical surface brightness of elliptical galaxies. In particular, a clear correlation exists between the shape and scale parameters (Fig. 3), with a shape very similar to that found for elliptical galaxies. The other parameters are also correlated, although with more dispersion than for ellipticals.

4.2 Constancy of the specific entropy

Once the scale parameter a_{eq} , the shape parameter ν and the central density ρ_0 are determined, we can compute the specific entropy s for the gas component of the cluster from equation (9). The gas mass can be computed from equation (6). We can then calculate the gas entropy $S = s M_{gas}$.

A plot of the gas entropy S as a function of the gas mass M_{gas} is shown in Fig. 6; a linear relation exists between the entropy and total mass of gas, implying that the specific entropy s is constant. The slope gives the value of $s = 34.5 \pm 1.3$. A remarkable characteristic of Fig. 6 is the very low dispersion of the points.

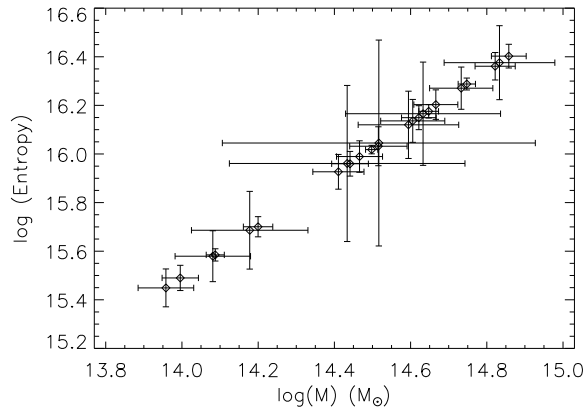


Figure 6: Relation between the gas entropy and mass.

4.3 Scaling relation between the cluster potential energy and the X-ray gas mass

The potential energy U_{pot} of the gas is displayed as a function of the gas mass in Fig. 7.

If we write this relation as $\log(U) - \alpha \log(M) = const$, we find a slope $\alpha = 1.72 \pm 0.05$, which is very close to the theoretical value of $5/3$.

This result confirms the hypothesis made for the formation of structures. The fact that elliptical galaxies and gas in clusters of galaxies verify the scaling law between potential energy and mass before mentioned is a strong argument in favour of the idea that self-gravitating structures are formed by processes where the conservation of energy and mass are verified.

4.4 Second order relations

Numerical simulations of elliptical galaxies formed in a hierarchical merging scheme show that the specific entropy slightly varies with mass, in a similar way as for observed galaxies (Márquez et al., 2000). This weak dependence has been interpreted as due to merging processes (Lima Neto et al., 1999).

We have searched for a similar relation in our sample of clusters. The plot of the gas specific entropy s versus the gas mass M_{gas} shown in Fig. 8 clearly reveals a linear relation between s and $\log(M_{gas})$. The gas specific entropy s is therefore a function of the gas mass. However, this is a second order relation compared to the more important relation $s = constant$ previously found. The difference with elliptical galaxies is that the slope in Fig. 8 is steeper for clusters than for ellipticals. Thus, if we write $s = s_0 + \beta \log(M)$, we find $\beta = 4.7 \pm 0.3$ for clusters and $\beta \simeq 1$ for ellipticals.

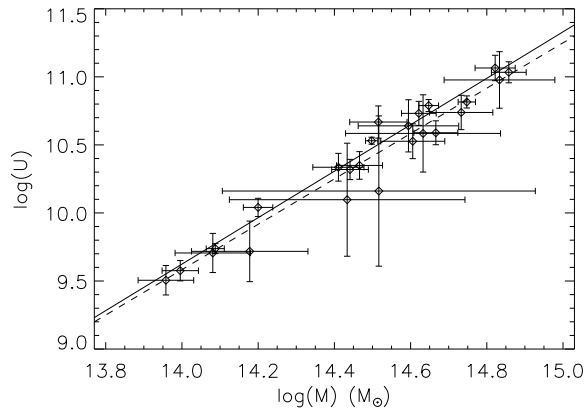


Figure 7: Scaling law between gas the potential energy and mass. The solid line corresponds to the best fit to the data and the dashed line is the theoretical curve (slope 5/3 in logarithmic units).

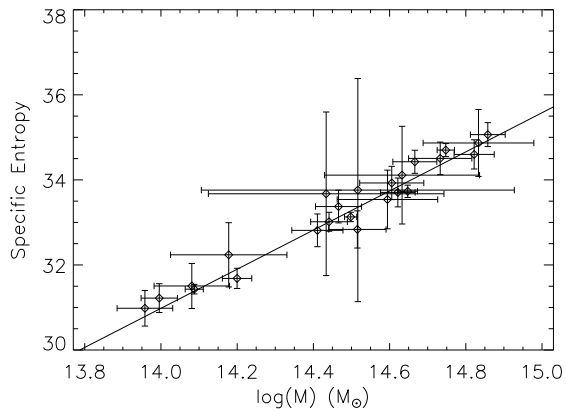


Figure 8: Relation between the gas specific entropy and mass. The straight line corresponds to the best fit slope $\beta = 4.7$.

5 Conclusions

The similarity of the relations found for the optical light distribution in elliptical galaxies and for the X-ray gas emission in clusters seems to confirm the hypothesis that the physical conditions prevalent when these self-gravitating systems were formed are comparable. These self-gravitating and almost dissipationless systems are likely to have evolved in a comparable way.

The more important dependence of the specific entropy with mass for clusters suggests that dissipating processes such as Bremsstrahlung emission ($L \propto M^2$) and cooling flows may play an important role as generators of entropy. Merging processes between clusters may also be of some importance.

The present work was carried out on a sample of 24 nearby clusters; the study of more distant objects could give us information on a possible dependence of specific entropy with redshift and on a possible evolution of the Sérsic scale parameter a . Such an analysis obviously requires a higher spatial resolution and sensitivity than those of ROSAT, and should be possible with XMM or Chandra.

References

1. Binney J., Tremaine S. 1987, "Galactic Dynamics", Princeton University Press
2. Ebeling H., Voges W., Böhringer H. et al. 1996, MNRAS 281, 799
3. Gerbal D., Lima Neto G.B., Márquez I., Verhagen H., 1997, MNRAS 285, L41
4. James F. 1984, CERN Program Library Long Writeup D506
5. Jang-Condell H., Hernquist L., 2001, ApJ 548, 68
6. Lanzoni B. 2000, PhD, Université Paris 7
7. Lima Neto G.B., Gerbal D., Márquez I., 1999, MNRAS 309, 481
8. Márquez I., Lima Neto G.B., Capelato H., Durret F., Gerbal D., 2000, A&A 353, 873
9. Márquez I., Lima Neto G.B., Capelato H., Durret F., Gerbal D., Lanzoni, B., 2001, A&A submitted
10. Mellier Y., Mathez G. 1987, A&A 175, 1
11. Sérsic J.L., 1968, "Atlas de galaxias australes, Observatorio Astronómico de Córdoba", Argentina
12. Snowden S. L., Kuntz K.D. US ROSAT Science Data Center, NASA/GSFC, 1994
13. Wu X.-P., Xue Y.-J., Fang L.-Z. 1999, ApJ 524, 22